Eur. Phys. J. B (2020) 93: 17
https://doi.org/10.1140/epjb/e2019-100576-6

THE EUROPEAN PHYSICAL JOURNAL B

Regular Article

Emergent SU(N) symmetry in disordered SO(N) spin chains*

Victor L. Quito[1,2], Pedro L.S. Lopes[3,4], José A. Hoyos[5,a], and Eduardo Miranda[6]

[1] Department of Physics and Astronomy, Iowa State University, Ames, Iowa 50011, USA
[2] Department of Physics and National High Magnetic Field Laboratory, Florida State University, Tallahassee, Florida 32306, USA
[3] Stewart Blusson Quantum Matter Institute, University of British Columbia, Vancouver, British Columbia V6T 1Z4, Canada
[4] Département de Physique, Institut Quantique and Regroupement Québécois sur les Matériaux de Pointe, Université de Sherbrooke, Sherbrooke, Québec J1K 2R1, Canada
[5] Instituto de Física de São Carlos, Universidade de São Paulo, C.P. 369, São Carlos, SP 13560-970, Brazil
[6] Instituto de Física Gleb Wataghin, Unicamp, Rua Sérgio Buarque de Holanda, 777, CEP 13083-859 Campinas, SP, Brazil

Received 27 November 2019 / Received in final form 17 December 2019
Published online 28 January 2020

Abstract. Strongly disordered spin chains invariant under the SO(N) group are shown to display random-singlet phases with emergent SU(N) symmetry without fine tuning. The phases with emergent SU(N) symmetry are of two kinds: one has a ground state formed of randomly distributed singlets of strongly bound pairs of SO(N) spins (a 'mesonic' phase), while the other has a ground state composed of singlets made out of strongly bound integer multiples of N SO(N) spins (a 'baryonic' phase). The established mechanism is general and we put forward the cases of $N = 2, 3, 4$ and 6 as prime candidates for experimental realizations in material compounds and cold-atoms systems. We display universal temperature scaling and critical exponents for susceptibilities distinguishing these phases and characterizing the enlarging of the microscopic symmetries at low energies.

1 Introduction

The process of symmetry breaking, as the energy of a given system is lowered, plays a central role in our current understanding of both high-energy physics (as in the standard model) and condensed matter physics (with universality and classification of phases) [1,2]. A less noticed (and explored) scenario is that of symmetry emergence, in which the lowering of the system's energy allows for ground states and excitations which are symmetric under a larger group of transformations than their corresponding microscopic Hamiltonian. A basic mechanism by which this can happen can be understood in the renormalization group framework by means of fixed points characterized by a symmetry which is broken only by irrelevant perturbations. There remains, nevertheless, a widespread lack of recognizable generic processes or patterns, so systems which realize this type of physics are found by trial and error (see Refs. [3–15] for examples). In scenarios dominated by disorder, the situation is even more clouded. It was in this context that, in reference [16], it was shown that generic disordered SU(2)-symmetric spin-1 chains exhibit emergent SU(3)-symmetric random-singlet phases (RSPs) [17]. There, it was also noted that in the pioneering work by Fisher on disordered XXZ spin-1/2 chains [18], there was also the emergence of SU(2) symmetric RSPs; SU(2) is explicitly broken down to U(1) in the microscopic XXZ Hamiltonian. What was *not* noted, however, is that in *both* cases the emergent SU(N) symmetry materialized out of systems with manifest SO(N) invariance, with $N = 3$ and 2, respectively.

This situation, which at first might be naively thought of as just a coincidence, uncovers, on the contrary, a consistent pattern. It is the aim of this letter to show that generic disordered magnetic chains invariant under the SO(N) group, in its defining vector representation, display emergent SU(N)-symmetric phases via a unified route for any $N \geq 2$; we denote this process by SO(N) $\overset{\text{emerg}}{\longrightarrow}$ SU(N). Our pattern of symmetry emergence contains two phases: (i) an obvious SU(N) generalization of the SU(2)-symmetric random singlet phase of the Heisenberg chain of reference [18], (ii) a phase whose ground state also consists of random SU(N)-symmetric singlets, but which are composed of kN original SO(N) 'spins', with k an arbitrary integer. Separating the two phases there is a critical point with manifest SU(N) symmetry. In the particular

* Contribution to the Topical Issue "Recent Advances in the Theory of Disordered Systems", edited by Ferenc Iglói and Heiko Rieger.

[a] e-mail: hoyos@ifsc.usp.br

Table 1. List of the most relevant SO(N)-symmetric one-dimensional models described by equation (5) with their possible physical realizations and the corresponding emergent symmetry in the limit of strong disorder.

Hamiltonian symmetry	Possible realizations	Emergent symmetry
SO(2)	Anisotropic spin-1/2 systems	SU(2)
SO(3)	Generic spin-1 systems	SU(3)
SO(4)	e_g orbitals in transition metal oxides	SU(4)
SO(6)	Cold fermionic alkaline-earth atoms	SU(6)

case of SO(3) $\stackrel{\text{emerg}}{\longrightarrow}$ SU(3) of reference [16] [previously interpreted as SU$(2)_{\text{spin-1}}$ $\stackrel{\text{emerg}}{\longrightarrow}$ SU(3)], particular versions of these phases were dubbed "mesonic" and "baryonic" random singlet phases, respectively. Furthermore, every one-dimensional RSP encountered so far [11,19–21] seems to find a counterpart in one of the permutation-symmetric multicritical points described by Damle and Huse [7,22], each one indexed by an integer n. The SO(N) baryonic RSPs we found realize all of these Damle-Huse points with $n=N$ in an extended phase (see also the discussion in Ref. [23]).

While SO(N) magnetism may sound exotic at first, such systems can be realized in several ways, either by exploiting explicit breaking of a larger SU(N) isotropy or, more interestingly, by taking advantage of the isomorphisms between orthogonal (so(N)) and unitary (su(N)) algebras at low N values. Some examples, summarized in Table 1, follow:

- The first two mentioned cases, that of the XXZ spin-1/2 Heisenberg chain [18] and of spin-1 bilinear and biquadratic Hamiltonians [16] can be realized in solid state [24] and, in principle, in cold atom systems [25,26], respectively. The former has a Hamiltonian with broken SU(2)-symmetry which, in fact, corresponds to an SO(2) symmetric Hamiltonian. The latter is realized explicitly as the most general SU(2)-symmetric Hamiltonian with spin-1 representations, but due to the algebra isomorphism so(3) $\sim$ su(2), it corresponds also to the most general SO(3)-symmetric Hamiltonian in the defining vector representation.
- Through the isomorphism so(4) $\sim$ su(2) $\otimes$ su(2), SO(4)-symmetric magnetism is realized by the well-known Kugel–Khomskii Hamiltonian [27], commonly used in the description of e_g orbitals in transition metal oxides [28], with su(2)-spin ($\mathbf{S}$) and su(2)-orbital ($\mathbf{T}$) degrees of freedom

$$H_{KK} = \sum_i \left[J_i \left(\mathbf{S}_i \cdot \mathbf{S}_{i+1} + \mathbf{T}_i \cdot \mathbf{T}_{i+1}\right) + 8D_i \left(\mathbf{S}_i \cdot \mathbf{S}_{i+1}\right)\left(\mathbf{T}_i \cdot \mathbf{T}_{i+1}\right)\right]. \quad (1)$$

- There are proposals to realize SU(N) magnetism with arbitrary N in fermionic alkaline-earth cold atomic systems in representations other than the fundamental one [29]. Exploiting the isomorphism so (6) $\sim$ su (4), disordered SU(4) magnetic chains in the self-conjugate representation realize an SO(6)-symmetric chain in its defining representation. In this case, according to our mechanism, disordered SU(4) symmetric chains would realize SU(4) $\stackrel{\text{emerg}}{\longrightarrow}$ SU(6).[1]
- Random SO($2S+1$) chains can, in fact, be designed by fine-tuning in *any* disordered rotation invariant spin-S system. Such generic spin-S chains have been previously studied by some of us [30], but the SO(N) phases of these systems were not characterized at that point.

We will first describe the general model and our results for the disordered SO(N) $\stackrel{\text{emerg}}{\longrightarrow}$ SU(N) mechanism. After that, we will give the finer technical details of our work.

2 Model and results

The $N(N-1)/2$ SO(N) generators [SO(N) 'spins'] will be denoted by L^{ab}, with a, b in the range $a=1,\ldots,N$ and $a<b$.[2] We will take them in the defining representation, which is spanned by a basis $|c\rangle$, $c=1,\ldots,N$. Each L^{ab} generates rotations in the ab plane. For $N=4$, for example, L^{23} rotates a four-dimensional vector in the $(2,3)$ Cartesian plane, while components 1 and 4 are kept fixed. In general,

$$iL^{ab}\left|c\right\rangle = \delta^{ac}\left|b\right\rangle - \delta^{bc}\left|a\right\rangle. \quad (2)$$

The L^{ab} operators obey the so(N) Lie algebra

$$\left[L^{ab}, L^{cd}\right] = i\left(\delta^{bc}L^{ad} + \delta^{ad}L^{bc} - \delta^{ac}L^{bd} - \delta^{bd}L^{ac}\right), \quad (3)$$

with $\mathrm{Tr}\left(L^{ab}L^{cd}\right) = 2\delta^{ac}\delta^{bd}$.

An SO(N)-symmetric Hamiltonian can be built as a sum over pairs of SO(N) spins (although 3-site terms are possible, we do not consider them here). In the defining representation, the most general pair term contains only bilinear and biquadratic terms [23,31]. In one dimension and considering only nearest-neighbor interactions we

[1] The proposal from reference [29] generates SU(N)-symmetric spin Hamiltonians, with arbitrary N, in perturbation theory in $1/U$ (where U is the usual Hubbard on-site interaction) in the Mott insulating limit. To lowest order, only the Heisenberg term appears. By symmetry, however, other SU(N)-invariant terms (biquadratic, etc.) are also allowed and appear in higher orders of perturbation theory. Systems which are closer to the Mott transition and at weaker interaction strengths should therefore be described by these more general SU(N) Hamiltonians.

[2] We can adhere to this convention if we define $L^{ab}=-L^{ba}$ whenever $a>b$.

have $H=\sum_i H_i$ where

$$H_i = J_i \mathbf{L}_i \cdot \mathbf{L}_{i+1} + D_i \left(\mathbf{L}_i \cdot \mathbf{L}_{i+1}\right)^2, \qquad (4)$$

where $\mathbf{L}_i \cdot \mathbf{L}_{i+1} = \sum_{a<b} L_i^{ab} L_{i+1}^{ab}$ and J_i, D_i are random couplings of ith link. For later convenience, we will recast H in terms of the linear combinations $K_i^{(1)} = J_i - \frac{N-2}{2} D_i$ and $K_i^{(2)} = \frac{N-2}{2} D_i$,

$$H_i = K_i^{(1)} \hat{O}_{i,i+1}^{(1)} + K_i^{(2)} \hat{O}_{i,i+1}^{(2)}, \qquad (5)$$

where $\hat{O}_{i,i+1}^{(1)} = \mathbf{L}_i \cdot \mathbf{L}_{i+1}$ and $\hat{O}_{i,i+1}^{(2)} = \mathbf{L}_i \cdot \mathbf{L}_{i+1} + \frac{2}{N-2} \left(\mathbf{L}_i \cdot \mathbf{L}_{i+1}\right)^2$.

We choose a parametrization of equation (5) in terms of the polar coordinates (r_i, θ_i) in the $\left(K_i^{(1)}, K_i^{(2)}\right)$ plane, so that $\tan\theta_i \equiv K_i^{(2)}/K_i^{(1)}$. For simplicity, we focus on random couplings $K_i^{(1)}$ and $K_i^{(2)}$ *with a fixed ratio throughout the chain*, i.e., $\theta_i = \theta\ \forall i$ (the general case is discussed elsewhere [23]). In the regime of strong disorder, RSPs are found at low energies. The phase is determined by θ, as displayed in a circle, see Figure 1a. The basins of attraction, delineated by the colors and arrows, are found via a strong-disorder renormalization group (SDRG) treatment [17,18,32–35]. The green and blue regions are both characterized by *infinite effective disorder* at long length scales [18]. More interestingly, both the blue and the green regions of Figure 1a correspond to phases with emergent SU(N) symmetry.

RSPs are characterized by a ground state formed by a collection of singlets. In the blue region, these random singlets are formed by spin pairs [SO(N) 'mesons'], as in the random Heisenberg chain studied by Fisher [18] (see Fig. 1b). In such a phase, long bonds of length L have strength of order $\Omega \sim \exp\left(-L^{\psi_M}\right)$ with $\psi_M = 1/2$. Low-energy excitations correspond to breaking the longest bonds into *free* SO(N) spins. At temperature $T = \Omega$, bonds of length $L > L_T \sim |\ln T|^{1/\psi_M}$ are broken and the density of free spins is $n(T) \sim L_T^{-1}$. Thermodynamic properties are then easily obtained: the spin linear susceptibility follows from Curie's law $\left[\chi^{(1)}\right]^{-1} \sim T/n(T) \sim T\left|\ln T\right|^{1/\psi_M}$, the entropy density is $s(T) \sim (\ln N)\, n(T)$ and the specific heat $c(T) = T\,(ds/dT) \sim |\ln T|^{-1-1/\psi_M}$. A hallmark of the infinite effective disorder is the wide distribution of correlation functions $C_{ij} = \langle \mathbf{L}_i \cdot \mathbf{L}_j \rangle$, so that, at $T=0$, its average value is $C_{ij}^{\text{av}} \sim (-1)^{i-j} |i-j|^{-2}$ whereas the typical (i.e., most probable) one is $\left|C_{ij}^{\text{typ}}\right| \sim \exp\left(-\left(|i-j|/\xi\right)^{\psi_M}\right)$, where ξ is a disorder-dependent length scale [36].

In the green region of Figure 1a, on the other hand, the ground state consists of a collection of singlets formed out of kN ($k = 1, 2, \ldots$) original SO(N) spins [SO(N) 'baryons'] as depicted in Figure 1c. The same relation between energy and length scales $\Omega \sim \exp\left(-L^{\psi_B}\right)$ holds,

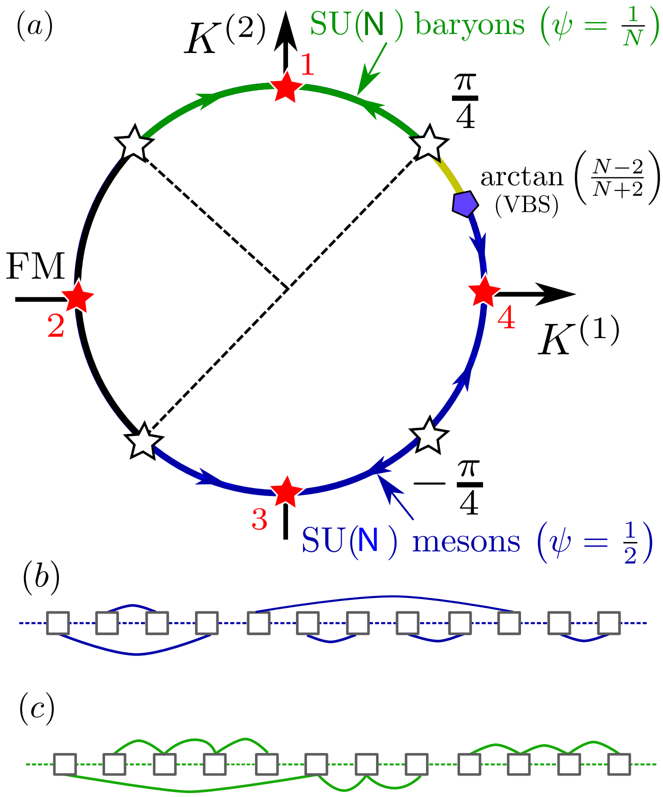

Fig. 1. (a) Phase diagram of the strongly-disordered one-dimensional SO(N)-symmetric Hamiltonian of equation (5). Points in the circle refer to the angle $\tan\theta \equiv K_i^{(2)}/K_i^{(1)}$, which is taken to be constant despite the randomness in $K_i^{(1,2)}$. The blue and the green regions realize two distinct random-singlet phases, *both* with emergent SU(N) symmetry. In the blue region, SU(N) singlets are built out of SO(N) 'spin' pairs ['mesons', shown in panel (b)]. The green region has SU(N) singlets made of kN 'spins' (with $k = 1, 2, \ldots$) ['baryons', shown in panel (c)]. The arrows indicate the renormalization group flow. Red and white stars represent stable and unstable fixed points, respectively. The black (for any N) and the yellow (for even N) regions are not addressed in this work.

but now the exponent is $\psi_B = 1/N$. Thermodynamic properties retain the same form described above but with $\psi_M \to \psi_B$. Note that the structure of these RSPs is the same as the Damle-Huse multicritical points [7,22].

The emergent SU(N) symmetry in each of these phases arises because, as it turns out, the strongly entangled SO(N) singlets, be they pairs or N-tuples, are also SU(N) singlets. Likewise, the original spins into which these singlets are broken at energies above zero also transform as SU(N) spins. As these two types of objects ultimately determine the low-energy properties, the latter will reflect this enhanced symmetry group. For example, the susceptibilities of the SU(N) operators (which can be constructed from linear *or bilinear* combinations of the SO(N) operators, as we will show) will also have the quoted behavior with the same exponent in each phase. The same is true of the correlation function distributions. These two types of phases and their properties had been described before by two of us in disordered spin chains with manifest SU(N) symmetry [19]. Here, they are realized asymptotically as emergent properties.

These are our main results. Their derivation relies on the application of an elegant Lie algebra machinery to the SDRG. In what follows we outline and motivate the results, relegating the full details to a longer and more pedagogic exposition [23].

3 SDRG details

The SDRG method is based on an iterative removal of degrees of freedom in real space following an energy hierarchy dictated by the largest local 2-site gap. Each iteration step consists of (i) the decimation of the pair with largest gap Ω by a projection of its Hilbert space onto its ground multiplet and (ii) the renormalization of the remaining couplings between this sub-space to the adjacent spins using perturbation theory. When applied sequentially, this process translates into a flow of the distribution of coupling constants. While the form of the Hamiltonian and the connectivity of the chain is preserved, new multiplets belonging to any one of the anti-symmetric SO(N) representations appear throughout the flow. As a consequence, the full characterization of the phases involves a flow of representation distributions.

Using equation (5), the decimation rules can be written in closed form [23]. Crucially, the decimations of the angles θ_i do not involve the radial variables r_i. Suppose the largest gap occurs between spins 2 and 3. If the ground multiplet of $H_{2,3}$ is not a singlet, it belongs to one of the int$(N/2)$ anti-symmetric representation of SO(N), and spins 2 and 3 are replaced by a new spin in that representation. The couplings in links 1 and 3 are renormalized according to

$$\tan\tilde{\theta}_{1,3} = \pm\tan\theta_{1,3}. \tag{6}$$

The choice of sign is determined by the representations being decimated as well as their ground state multiplet [23]. If the ground multiplet of $H_{2,3}$ is a singlet, spins 2 and 3 are effectively removed. In this case, a new coupling between spins 1 and 4 is created with [23]

$$\tan\tilde{\theta} = -\left(\frac{N+2}{N}\right)\frac{\frac{N-2}{N+2}-\tan\theta_2}{1-\tan\theta_2}\tan\theta_1\tan\theta_3. \tag{7}$$

In the blue mesonic region of Figure 1a, the ground multiplets are always singlets and it follows trivially from equation (7) that $\theta = 0$ and $-\pi/2$ (points 3 and 4 of the Figure) and $\theta = -\pi/4$ are fixed points of the flow. The same equation can be used to show that points 3 and 4 are stable whereas $\theta = -\pi/4$ is unstable.

In the green baryonic region of Figure 1a both types of decimations occur and the analysis is more involved. The pair of angles $\theta = \pm\pi/2$ taken together are fixed points and singlets are formed out of kN $(k = 1, 2, \ldots)$ of SO(N) spins. There are several paths by which this can happen and an illustrative example is shown in Figure 2 for SO(4). In this case, the RG flow involves two anti-symmetric

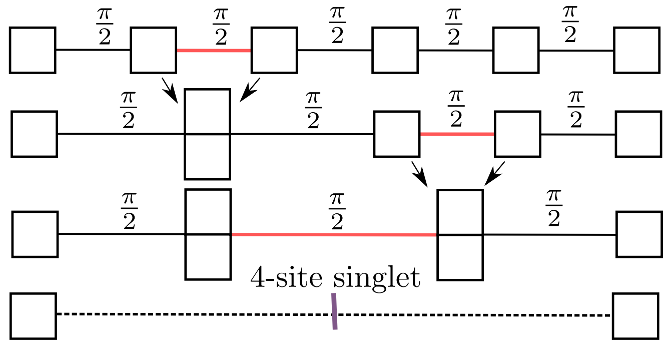

Fig. 2. An example of singlet formation for SO(4) at the fixed point 1 of Figure 1a, with θ_i indicated on each bond.

representations depicted by Young tableaux with 1 or 2 stacked boxes. Note how the angle can switch back and forth from $\pi/2$ to $-\pi/2$ depending on the representations involved. This is the fixed point 1 in Figure 1a. A stability analysis shows that point 1 is a stable fixed point. Similarly, the extremities of the green region $\theta = \pi/4$ and $\theta = 3\pi/4$ are unstable fixed points since, crucially, they lead to Hamiltonians with exact SU(N) symmetry and this symmetry is preserved by the SDRG flow.

We now show that the SO(N)-symmetric Hamiltonian of equation (5) can be viewed as an SU(N)-anisotropic problem. The N^2-1 generators $\{\Lambda_i\}$ of the fundamental representation of the SU(N) group are traceless Hermitian matrices, normalized as $\mathrm{Tr}[\Lambda_i^{(a)}\Lambda_j^{(b)}] = 2\delta^{ab}\delta_{ij}$. We can break this set in a subset of $N(N-1)/2$ purely imaginary anti-symmetric matrices, the generators of SO(N), and another subset of $N(N+1)/2-1$ real traceless symmetric ones, which are SO(N) second-rank tensors [see the form of $\hat{O}^{(2)}_{i,i+1}$ after Eq. (5)]. The Hamiltonian (5) is then equivalent to an SU(N)-anisotropic Hamiltonian,

$$H_i = K_i^{(1)}\sum_{a=1}^{d_{\mathrm{SO}(N)}}\Lambda_i^{(a)}\Lambda_{i+1}^{(a)} + K_i^{(2)}\sum_{a=d_{\mathrm{SO}(N)}+1}^{N^2-1}\Lambda_i^{(a)}\Lambda_{i+1}^{(a)}, \tag{8}$$

with $d_{\mathrm{SO}(N)} = \frac{N(N-1)}{2}$. We can immediately find the expected SU(N)-symmetric points: $K_i^{(1)} = \pm K_i^{(2)}$. That the choice with a minus sign is also SU(N)-symmetric can be seen from the transformation $\Lambda_i^{(a)} \to -\Lambda_i^{(a)*} \equiv \tilde{\Lambda}_i^{(a)}$ on every other chain site, which changes an SU(N) representation into its conjugate and absorbs the minus sign. This case corresponds to having SU(N) (anti-) fundamental representations on odd (even) sites.

The location of these angular fixed points sets the topology of the flow, as shown by the arrows in Figure 1a. Although the θ-distribution starts as a delta function, it broadens under the SDRG flow. The existence of the stable fixed points, however, forces the distribution to narrow back down to a delta function at one of the points 1, 3 or 4. Point 2 and its associated black region are outside the scope of this paper as symmetric representations of SO(N) are generated by the flow. The yellow region between the generalized AKLT point $\theta_{\mathrm{VBS}} = \arctan\left[(N-2)/(N+2)\right]$ (blue pentagon) [37] and $\pi/4$ flows to the fixed point 4 for odd N. For even N, the procedure becomes ill-defined in this region, and our method cannot be applied [23].

The renormalization of radial variables depends explicitly on the representations being decimated as well as the effective ones being introduced. A systematic derivation of such rules will be given elsewhere [23], but up to prefactors, the rules are the ones derived in reference [7]. The distribution of r_i broadens without limit and flows to an infinite disorder form given by $P(r) \sim r^{\alpha_i(\Omega)-1}$. Here $\alpha_i(\Omega) = \left(\psi_i^{-1} - 1\right)/|\ln \Omega|$, $i = B$ or M in the green or blue region, respectively, and Ω is the decreasing cutoff of the distribution [16,18,23,33].

In the blue region, adjacent spins always form a singlet and no other representation appears in the flow. The ground state structure is shown in Figure 1b. In contrast, in the green region decimations with ground multiplets belonging to any one of the $\mathrm{int}(N/2)$ antisymmetric representations of SO(N) are generated. After an initial transient, each one of them is equally populated in the renormalized system.[3] A singlet only forms out of kN ($k = 1, 2, \ldots$) SO(N) spins, leading to the ground state structure in Figure 1c. The different singlet structures lead to different physical properties at finite energies, as discussed above. The apparently intricate combinations leading to singlet formation out of kN SO(N) spins can be easily understood at the exact SU(N) point $\theta = \pm\pi/4$: only with kN SU(N) fundamentals can one form an SU(N) singlet [19]. The stable fixed points that attract the flow are adiabatically connected to these SU(N) points and have the same ground state structure.

The emergent SU(N) symmetry, as mentioned, relies on the fact that free spins and frozen singlets, the building blocks of the renormalized system, transform as SU(N) fundamentals and singlets, respectively. If we now recall that some of the SU(N) generators $\Lambda_i^{(a)}$ with $a \in \left[N(N-1)/2+1, N^2-1\right]$ are actually 2nd-rank SO(N) tensors (see Eqs. (5) and (8)), it follows that susceptibilities and correlation functions built with these quadratic SO(N) operators are governed by the same power laws as those of the SO(N) generators. Measuring SO(N) susceptibilities may sound as a challenging task. Yet, we point that this can be envisaged at least for the case of $N = 3$. In this case these susceptibilities are just regular magnetic susceptibilities for spin-1 operators [16]. The susceptibilities for 2nd rank operators in this case are nothing but quadrupolar susceptibilities; protocols for their measurements have recently been proposed at least in two dimensions by considering cross responses between magnetic probes and strain [38].

4 Conclusions

Our study of random SO(N)-symmetric chains unveils a unified mechanism of symmetry emergence in a large and diverse set of realizable physical situations. Some possible realizations had been previously studied ($N = 2, 3$) but new ones ($N = 4, 6$) are here introduced. Crucial to the mechanism is the existence of explicit SU(N)-symmetric points in the parameter space whose ground states are adiabatically connected (no local-gap closing) to those of a finite region: symmetry emergence requires no fine tuning. Disorder is the ingredient responsible for filtering, from the set of SO(N) representations, those which find correspondence in the SU(N) group.

[3] With one exception: for even N, the self-conjugate representation is half as likely as any of the others.

We thank Gabe Aeppli for discussions. VLQ and PLSL contributed equally to this work. VLQ acknowledges financial support from the National High Magnetic Field Laboratory through grant DMR-1157490, the State of Florida and the Aspen Center for Physics, supported by NSF grant PHY-1607611, for hospitality. PLSL is supported by the Canada First Research Excellence Fund. JAH and EM acknowledge financial support from FAPESP, CNPq and Capes.

Author contribution statement

V.L.Q. and P.L.S.L. performed the necessary calculations, with inputs of E.M. and J.A.H. All the authors participated in the discussions of the results. E.M. and J.A.H. suggested the connections with higher-order susceptibilities. The manuscript was written with the equal collaboration of all authors.

References

1. P.W. Anderson, *Basic notions of condensed matter physics* (Benjamin-Cummings, Melon-Park, California, 1984)
2. R.B. Laughlin, D. Pines, Proc. Natl. Acad. Sci. **97**, 28 (2000)
3. A.B. Zamolodchikov, Int. J. Mod. Phys. A **4**, 4235 (1989)
4. A. Rahmani, X. Zhu, M. Franz, I. Affleck, Phys. Rev. Lett. **115**, 166401 (2015)
5. J. Schmalian, C. Batista, Phys. Rev. B **77**, 094406 (2008)
6. R. Coldea, D.A. Tennant, E.M. Wheeler, E. Wawrzynska, D. Prabhakaran, M. Telling, K. Habicht, P. Smeibidl, K. Kiefer, Science **327**, 177 (2010)
7. K. Damle, D.A. Huse, Phys. Rev. Lett. **89**, 277203 (2002)
8. T. Senthil, A. Vishwanath, L. Balents, S. Sachdev, M.P.A. Fisher, Science **303**, 1490 (2004)
9. T. Grover, D.N. Sheng, A. Vishwanath, Science **344**, 280 (2014)
10. C.D. Batista, G. Ortiz, Adv. Phys. **53**, 1 (2004)
11. L. Fidkowski, H.-H. Lin, P. Titum, G. Refael, Phys. Rev. B **79**, 155120 (2009)
12. P. Chen, Z.-L. Xue, I.P. McCulloch, M.-C. Chung, C.-C. Huang, S.-K. Yip, Phys. Rev. Lett. **114**, 145301 (2015)
13. E. Zohar, J.I. Cirac, B. Reznik, Rep. Prog. Phys. **79**, 014401 (2016)
14. C. Itoi, M.-H. Kato, Phys. Rev. B **55**, 8295 (1997)
15. H.-H. Lin, L. Balents, M.P.A. Fisher, Phys. Rev. B **58**, 1794 (1998)
16. V.L. Quito, J.A. Hoyos, E. Miranda, Phys. Rev. Lett. **115**, 167201 (2015)
17. S.K. Ma, C. Dasgupta, C.K. Hu, Phys. Rev. Lett. **43**, 1434 (1979)

18. D.S. Fisher, Phys. Rev. B **50**, 3799 (1994)
19. J.A. Hoyos, E. Miranda, Phys. Rev. B **70**, 180401 (2004)
20. N.E. Bonesteel, K. Yang, Phys. Rev. Lett. **99**, 140405 (2007)
21. L. Fidkowski, G. Refael, N.E. Bonesteel, J.E. Moore, Phys. Rev. B **78**, 224204 (2008)
22. K. Damle, Phys. Rev. B **66**, 104425 (2002)
23. V.L. Quito, P.L.S. Lopes, J.A. Hoyos, E. Miranda, Phys. Rev. B **100**, 224407 (2019)
24. R. Toskovic, R. van den Berg, A. Spinelli, I.S. Eliens, B. van den Toorn, B. Bryant, J.-S. Caux, A.F. Otte, Nat. Phys. **12**, 656 (2016)
25. J.J. García-Ripoll, M.A. Martin-Delgado, J.I. Cirac, Phys. Rev. Lett. **93**, 250405 (2004)
26. A. Imambekov, M. Lukin, E. Demler, Phys. Rev. A **68**, 063602 (2003)
27. K.I. Kugel, D.I. Khomskii, Sov. Phys. Usp. **25**, 231 (1982)
28. Y. Tokura, N. Nagaosa, Science **288**, 462 (2000)
29. A.V. Gorshkov, M. Hermele, V. Gurarie, C. Xu, P.S. Julienne, J. Ye, P. Zoller, E. Demler, M.D. Lukin, A.M. Rey, Nat. Phys. **6**, 289 (2010)
30. V.L. Quito, J.A. Hoyos, E. Miranda, Phys. Rev. B **94**, 064405 (2016)
31. H.-H. Tu, G.-M. Zhang, T. Xiang, Phys. Rev. B **78**, 094404 (2008)
32. C. Dasgupta, S.-K. Ma, Phys. Rev. B **22**, 1305 (1980)
33. D.S. Fisher, Phys. Rev. B **51**, 6411 (1995)
34. F. Iglói, C. Monthus, Phys. Rep. **412**, 277 (2005)
35. F. Iglói, C. Monthus, Eur. Phys. J. B **91**, 290 (2018)
36. J.C. Getelina, J.A. Hoyos, Eur. Phys. J. B **93**, 2 (2019)
37. I. Affleck, T. Kennedy, E.H. Lieb, H. Tasaki, Phys. Rev. Lett. **59**, 799 (1987)
38. A. Patri, A. Sakai, S. Lee, A. Paramekanti, S. Nakatsuji, Y.B. Kim, Nat. Commun. **10**, 4092 (2019)